ELSEVIER

Journal of Electroanalytical Chemistry 427 (1997) 113–121

JOURNAL OF ELECTROANALYTICAL CHEMISTRY

Electroanalytical study on the ion-exchange voltammetric behaviour of Hg(II) at Tosflex®-coated glassy carbon electrodes

Ligia Maria Moretto, Gian Antonio Mazzocchin, Paolo Ugo *

Department of Physical Chemistry, University of Venice, Calle Larga S. Marta 2137, I-30123 Venice, Italy

Received 17 June 1996; revised 11 October 1996

Abstract

The cyclic voltammetric behaviour of $HgCl_4^{2-}$ at glassy carbon electrodes coated with a thin film of Tosflex® IE-SA 48 (a perfluorinated anion exchanger) is studied.

Concerning the reduction of $HgCl_4^{2-}$ preconcentrated in the coating, a relevant positive shift in reduction peak potentials is observed, both when increasing the $HgCl_4^{2-}$ solution concentration and decreasing the scan rate. The analysis of the voltammograms indicates that an irreversible reduction process is occurring. A remarkable positive shift in peak potentials with respect to bare electrodes is also observed.

All experimental evidence obtained agrees with the formation of a metal phase, namely Hg^0, whose deposition is highly favoured by the presence of the coating, as a consequence both of preconcentration effects and of the decrease in diffusion coefficients related to the ion-exchange incorporation.

As far as the reoxidation of deposited Hg^0 is concerned, the study of the effect of the scan rate, the analyte solution concentration and the loading of chloride anions in the coating indicates that the reversible oxidation to an insoluble calomel deposit occurs at high Hg^0 and low Cl^- loadings. The formation of calomel is confirmed also by ex situ X-ray diffractometric measurements. On the contrary, low Hg^0 and high Cl^- loadings within the coating favour the disproportionation of the calomel formed and the complete regeneration of the modified electrode. © 1997 Elsevier Science S.A.

Keywords: Mercury(II); Ion-exchange; Glassy carbon electrodes; Tosflex® coating

1. Introduction

The application of polymer-modified electrodes for developing more selective and sensitive ion-exchange voltammetric methods is increasing in popularity [1]. However, many fundamental aspects related to the preconcentration and detection of very low levels of electroactive species and/or their metallic reduction products remain quite obscure. In fact, the detailed analysis of the ion-exchange voltammetric behaviour of incorporated electroactive species has been developed mainly for the simpler cases of reversible charge transfer processes involving redox partners which are both incorporated and can diffuse into the polymer phase [2–4].

Some papers which present the use of new ion-exchange anodic-stripping methods for determining trace electroactive species via ion-exchange incorporation, following reduction to the metal and final detection via anodic stripping at the electrode|polymer interface have been published recently [5–11]. Such an approach shows unquestionable advantages as far as improvement of selectivity, sensitivity and detection limits are concerned; however, the interpretation of the role of the coating in determining changes in relevant electrochemical parameters such as peak potentials and currents is sometimes oversimplified. Models developed for simpler cases [12], are often extrapolated to the more complex situation of the deposition and stripping of a metal at a polymer-coated electrode.

In a recent paper we showed that the ion-exchange anodic-stripping approach can be exploited successfully to determine trace mercury in chloride media at glassy carbon electrodes coated with Tosflex®, a perfluorinated anion exchanger, with a detection limit as low as 4×10^{-11} M [13]. At the chloride concentration typical of seawater

* Corresponding author.

PII S0022-0728(96)05004-8

(0.55 M), $HgCl_4^{2-}$ is in fact the prevailing inorganic mercury(II) species [14], which can be preconcentrated by anion-exchangers such as Tosflex®. Moreover, the use of Tosflex®-coated electrodes allows one to eliminate the interference due to the presence of Cu^{2+} even in a 100-fold molar excess. In that study, it was observed that the presence of the polymeric coating changed some of the characteristics of the voltammetric pattern dramatically; however a detailed analysis of the observed phenomena was not performed, being outside the aims of that work.

In the present paper we report the results of a mechanistic investigation aimed to analyse and to understand the electrochemical behaviour of $HgCl_4^{2-}$ preconcentrated by ion-exchange at Tosflex®-modified glassy carbon electrodes. Attention will focus in particular on the role played by the coating in making the deposition of mercury metal much easier than at unmodified electrodes as well as in determining the mechanism of the oxidative stripping of such a deposit.

2. Experimental

2.1. Chemicals

All chemicals used were of analytical reagent grade. Milli-Q water was used throughout for preparing supporting electrolyte solutions. $Hg(NO_3)_2$ solutions were prepared by proper dilution of a mercury atomic absorption standard solution (Aldrich).

Aqueous alcoholic solutions (water + methanol + 2-propanol, 1:1:1) of Tosflex® IE-SA 48 polymer were prepared from the thick solid membrane, obtained from Tosoh Soda, using the method of Dunsch et al. [15].

The structural formula of Tosflex IE-SA 48 is

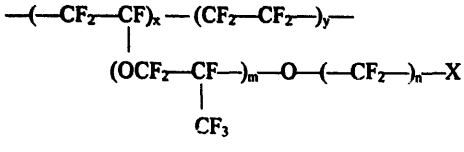

where $m = 0–1$, $n = 1–5$ and X = anion-exchange unit.

The filtered solution had a concentration of about 2.5% (w/v).

Determination of the ion-exchange capacity of the thick commercial membrane by titration of the chloride released after treatment with excess sulphate, gave an equivalent molar mass of Tosflex® IE-SA 48 of 1850 g mol^{-1}; this datum, together with the measurement of the thickness of coatings prepared by deposition of known amounts of polymer solutions (see below), gave a concentration of ion-exchange sites in the coating equivalent to 1 mol dm^{-3}.

2.2. Apparatus and procedures

All electroanalytical measurements were carried out at room temperature (22 ± 1°C) under a nitrogen atmosphere. A conventional single-compartment cell equipped with a platinum coil counter electrode and an Ag|AgCl reference electrode was employed.

The working electrodes were a PTFE-shrouded glassy carbon disk (area 0.2 cm^2) or a gold disk electrode, both polished to a mirror finish with graded alumina powder.

Generally, Tosflex®-coated electrodes were prepared by droplet evaporation of 3 μl of 2.5% (w/v) Tosflex solution deposited with a microsyringe on a mirror-polished disk electrode. The evaporation of the solvent was performed in a methanol atmosphere to ensure a slow evaporation rate. The average value for the thickness of the coating, measured with an Alfa step profilometer (Tencor, Mountain View, CA) was 1.8 μm. Wetting of the coating with the supporting electrolyte solution did not change this thickness significantly. Coatings of different thicknesses (1.2 and 3.0 μm) were prepared by properly changing the volume of Tosflex® solution deposited on the electrode surface.

Electrochemical measurements were carried out with an EG&G PAR Model 273 programmable potentiostat controlled by a personal computer via EG&G PAR M270 software.

IR-drop compensation was used in the measurements, however with some care since it was observed that the use of *IR*-drop compensation can cause the formation of insoluble calomel on the electrode surface, even before the reoxidation scan (see below). This was attributed to oscillations in the applied potential when using high compensation levels. If this was the case, the measurement was repeated using a new electrode and suitably lowering the compensation level as well as adjusting the undershoot parameter; sometimes, the required lowering of the compensation level was such that it did not ensure the full compensation of *IR* drop.

Digital simulations were carried out using DIGISIM 2.0 (Bas Inc.), a cyclic voltammetric simulation program, running on an HP 735/90 CPU Pentium computer.

The ex situ X-ray diffractometric measurements were performed with a θ–2θ powder goniometer in the Bragg–Brentano parafocusing geometry, using the radiation Cu Kα ($\lambda = 1.54178$ Å) and a graphite monochromator in the diffracted beam. Front slits of 6 mm were reduced laterally in order to direct the beam only to the electrode surface. The values of angles 2θ exploited varied from 20° to 50°.

3. Results and discussion

3.1. Reduction of $HgCl_4^{2-}$ at Tosflex®-modified electrodes

Fig. 1 shows the cyclic voltammetric patterns recorded at different scan rates, using a Tosflex®-coated glassy

carbon electrode dipped in $HgCl_4^{2-}$ solutions. The voltammograms are recorded after equilibration of the modified electrode with the electrolyte solution, i.e. when no change of the voltammograms is observed with time. The equilibration process, which takes about 30 min in unstirred solutions, corresponds to the achievement of the ion-exchange equilibrium (Eq. (1)) [13]:

$$2Cl_p^- + HgCl_{4s}^{2-} \rightleftarrows HgCl_{4p}^{2-} + 2Cl_s^- \quad (1)$$

Subscripts p and s refer to concentrations in the polymer and in the solution phase respectively.

The ion-exchange equilibrium (Eq. (1)) is characterised by a selectivity coefficient $K_{Cl}^{Hg} = [HgCl_4^{2-}]_p[Cl^-]_s^2/[HgCl_4^{2-}]_p[Cl^-]_s^2$ of 5×10^3, while the distribution coefficient $k_D = [HgCl_4^{2-}]_p/[HgCl_4^{2-}]_s$, measured in 0.5 M NaCl, is 1.1×10^4 [13]. The effectiveness of the ion-exchange preconcentration agrees with the experimental observation that voltammetric peak currents recorded at modified electrodes are roughly 20 times higher than currents recorded in the same experimental conditions at bare electrodes.

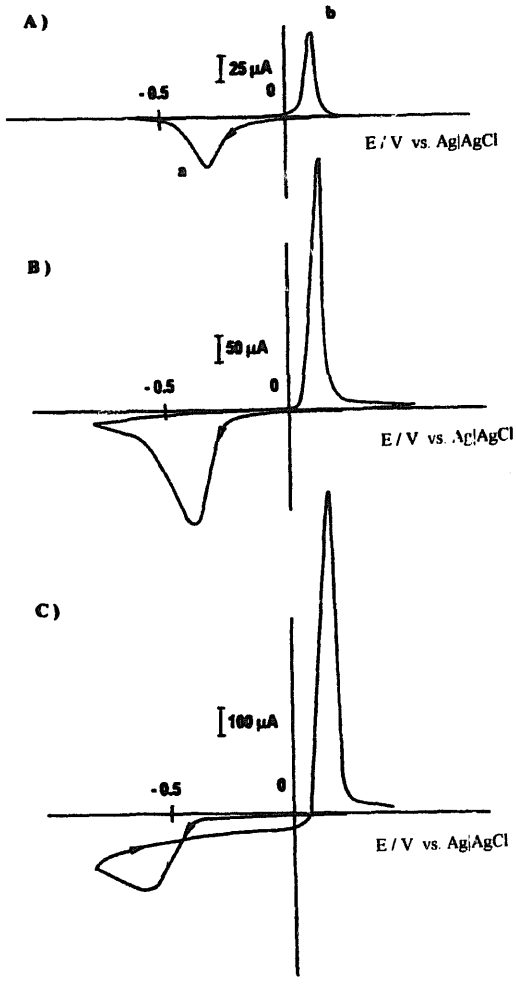

Fig. 1. Cyclic voltammograms recorded at Tosflex®-coated glassy carbon electrodes in 5×10^{-5} M Hg(II) at scan rates of: (A) 10 mV s^{-1}, (B) 50 mV s^{-1} and (C) 200 mV s^{-1}. Supporting electrolyte: 0.5 M NaCl + 10^{-2} M HCl.

Table 1
Scan rate dependence of potential values of peak (a) at Tosflex®-coated glassy carbon electrodes; electrolyte solution: 5×10^{-5} M Hg(II) + 0.5 M NaCl + 10^{-2} M HCl

v/mV s^{-1}	E_p/mV	$(E_p - E_{p/2})$/mV
10	−310	65
50	−380	70
100	−430	80
200	−570	90

The voltammogram reported in Fig. 1(C) shows that a cross-over characterises the voltammetric pattern recorded at relatively high scan rates (200 mV s^{-1}).

The current of peak (a) is linearly dependent on v for scan rates < 50 mV s^{-1}; this indicates a surface-confined process which corresponds to the reduction of all the $HgCl_4^{2-}$ incorporated in the coating during the voltammetric scan (finite diffusion) [16]. In contrast, the voltammograms recorded at scan rates ≥ 50 mV s^{-1} show a dependence of the peak currents on the square root of the scan rate, which is typical of semi-infinite linear diffusion [17].

A rough estimate of the apparent diffusion coefficient of $HgCl_4^{2-}$ incorporated in the polymer layer can be obtained by considering that the scan rate of the transition between finite and semi-infinite linear diffusion is related to the film thickness ϕ (= 1.8 μm, see Section 2) by the relationship $(D_{app}RT/Fv)^{1/2} = \phi$ [18]. Proper numerical substitutions suggest an expected D_{app} value in the 10^{-8} cm^2 s^{-1} range. As shown below, a more precise evaluation of D_{app} in this case is complicated by the irreversibility of the reduction process and by the fact that the deposition of metallic mercury, which is the final reduction product [13], changes the electrode area during the measurement time.

As shown by data listed in Table 1, in the range of scan rates explored, the potential of peak (a) shifts linearly (about 120 mV for a one decade increase in v) towards more negative potential values while increasing the scan rate. Table 1 shows also that quite large $E_p - E_{p/2}$ values, which increase slightly with the scan rate, characterise the reduction process. Because of problems in performing the full compensation of *IR* drop (see Section 2) it is not possible to exclude that residual uncompensated resistance can be the cause of such an increase.

Anyway, both the negative shift in E_p values with the scan rate and the high $(E_p - E_{p/2})$ values indicate that the electrochemical reduction of the ion-exchanged $HgCl_4^{2-}$ to metallic mercury which takes place at peak (a), is irreversible; however, it displays some peculiarities which need further interpretation.

First of all, the appearance of the cross-over at high scan rates can be explained taking into account that the deposition of mercury on carbon is much more energy demanding than the deposition of mercury on mercury, the first process being affected by higher overpotential [19,20].

If the electrolysis time is short (high scan rates) only a little metallic mercury is deposited and the more energy demanding formation of the first metallic nuclei, which reflects in the appearance of the cross-over [21], is the process observed. On the contrary, at higher electrolysis time, i.e. at slower scan rates or at higher concentrations (see below), in the experimental time scale enough mercury is deposited, so that the less energy demanding deposition of mercury on mercury becomes the prevailing process.

The role of the nature of the electrode material in determining the reduction potential of Hg(II) at coated electrodes is confirmed by the voltammograms recorded at gold electrodes. As shown in Fig. 2(A), the well known higher reversibility of Hg(II) reduction at gold electrodes [22] is reflected in a dramatic positive shift in the reduction peak potential at Tosflex®-coated gold electrodes with respect to Tosflex®-coated glassy carbon electrodes. Quite interestingly, comparison with Fig. 2(B), obtained at bare gold, indicates that the voltammetric pattern recorded at Tosflex®-coated gold electrodes is simpler and displays some features different from those which characterise the pattern at bare gold electrodes, the latter being complicated by the occurrence of complex Hg–Au interactions [23–25].

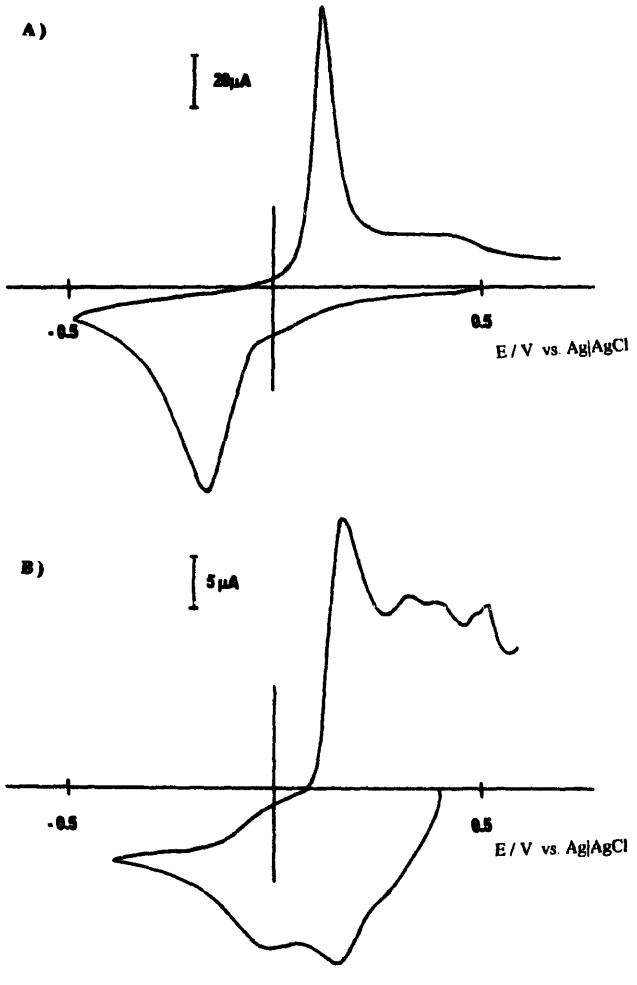

Fig. 2. Cyclic voltammograms recorded at $50\,mV\,s^{-1}$ in 0.5 M NaCl + 10^{-2} M HCl: (A) Tosflex®-coated gold electrode in 1×10^{-5} M Hg(II); (B) bare gold disk electrode in 2.5×10^{-4} M Hg(II).

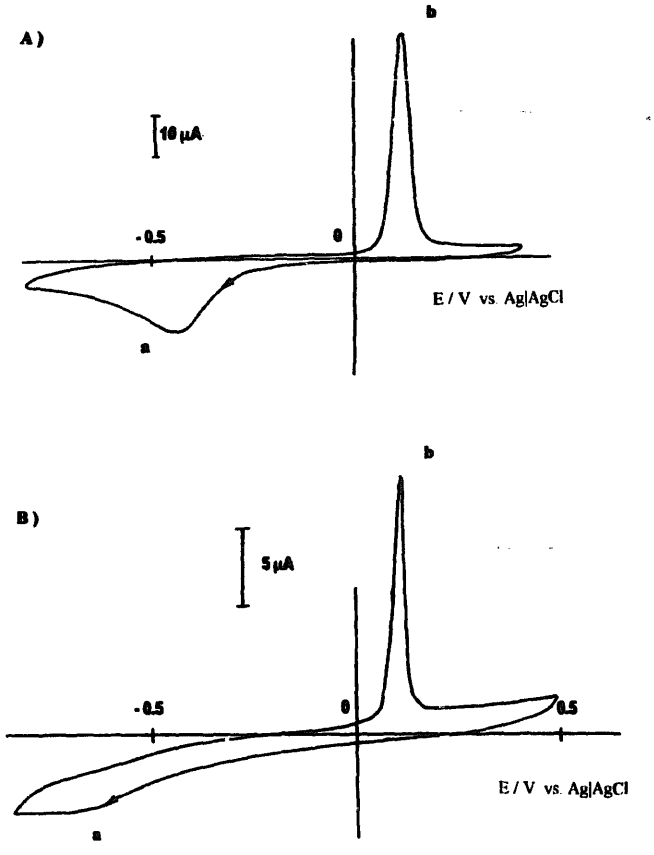

Fig. 3. Cyclic voltammograms recorded at $50\,mV\,s^{-1}$ in 0.5 M NaCl + 10^{-2} M HCl: (A) Tosflex®-coated glassy carbon electrodes in 5×10^{-6} M Hg(II); (B) bare glassy carbon in 5×10^{-5} M Hg(II).

Measurements carried out at glassy carbon electrodes coated with different thicknesses of Tosflex® polymer (namely 1.2 and 3.0 μm, in addition to the generally used 1.8 μm thickness), do not show any relevant influence of such a parameter on the features of the voltammograms, at least as far as semi-infinite planar diffusion conditions hold ($v \geq 50\,mV\,s^{-1}$). This agrees with the expectation that diffusion-controlled peak currents and potentials are influenced by the concentration of $HgCl_4^{2-}$ within the coating rather than by the overall amount incorporated.

Really, the reduction process which generates Hg^0 is expected to follow an EE pathway [26] in which the first chemical step is the one-electron irreversible reduction of Hg(II) followed by the further one-electron reversible reduction to metallic mercury; for the case under study the following reaction sequence is expected to occur:

$$2HgCl_4^{2-} + 2e^- \rightarrow Hg_2Cl_2 + 6Cl^- \quad (2)$$

$$Hg_2Cl_2 + e^- \rightleftarrows 2Hg^0 + 2Cl^- \quad (3)$$

with $E°(2) > E°(3)$ [26].

Fig. 3(A) shows the effect of a decrease in Hg(II) solution concentration on the response obtained at a Tosflex®-coated glassy carbon electrode. A negative shift in

peak potentials and a slight increase in $(E_p - E_{p/2})$ values are observed with respect to the voltammogram shown in Fig. 1(B). Such changes agree with the involvement of a reduction process which gives a metal phase as the final product. For such cases, when semi-infinite planar diffusive control holds, the potential of the reduction peak is given by Eq. (4) [27]:

$$E_p = \text{const} + RT/nF \ln c - RT/\alpha n_\alpha F \times \left[0.789 + \ln(D^{1/2}/k^\circ) + \ln(\alpha n_\alpha F v/RT)^{1/2}\right] \quad (4)$$

In our case, c is the concentration of electroactive species incorporated into the polymer coating, D is the relevant apparent diffusion coefficient in the coating (D_{app}) and all other symbols have their usual meaning.

Fig. 3(B) shows the voltammetric pattern obtained at a bare glassy-carbon electrode in a 5×10^{-5} M $HgCl_4^{2-}$ solution. The comparison of this voltammogram with the one shown in Fig. 1(B) reveals that the reduction peak potential at the modified electrode is consistently more positive than at the unmodified electrode.

In principle, shifts in peak potentials between modified and unmodified electrodes are related to a combination of different factors which include:

1. permselectivity of the coating [2] and preconcentration of the electroactive species;
2. role of the coating in changing the energetics involved in the deposition of a metal phase [19];
3. changes in diffusion coefficients of the electroactive species between solution and polymer phases.

The occurrence of such multiple effects is supported first of all, by the evidence that the observed shift in peak potentials, differs from the shift expected on the basis of the permselectivity effect alone (see for instance Eq. (7) in Ref. [12]). One possible explanation (but not the only one) is given by the dependence of peak potentials on the concentration of the electroactive species discussed above, (see Eq. (4)); the local increase in the $HgCl_4^{2-}$ concentration, related to the ion-exchange preconcentration process, reflects in fact in a positive shift in peak potentials. Moreover, it cannot be excluded that the presence of the coating can influence the energetics of the deposition by changing the real potential of the electrode surface, as adsorption phenomena do [19].

Another important point is that also changes in diffusion coefficients between solution and polymer phase cannot be neglected; this is evidenced by the dependence of E_p on D expressed by Eq. (4). Unfortunately, as shown above, for the case under study it is not possible to measure exactly the apparent diffusion coefficient of $HgCl_4^{2-}$ in the coating. However, it must be noted that the estimated D_{app} value around 10^{-8} cm^2 s^{-1} is roughly two orders of magnitude lower than the diffusion coefficient in solution [28]. Such a relevant decrease in diffusion coefficient values can really constitute an important contribution to the positive shift in peak potential values experimentally observed.

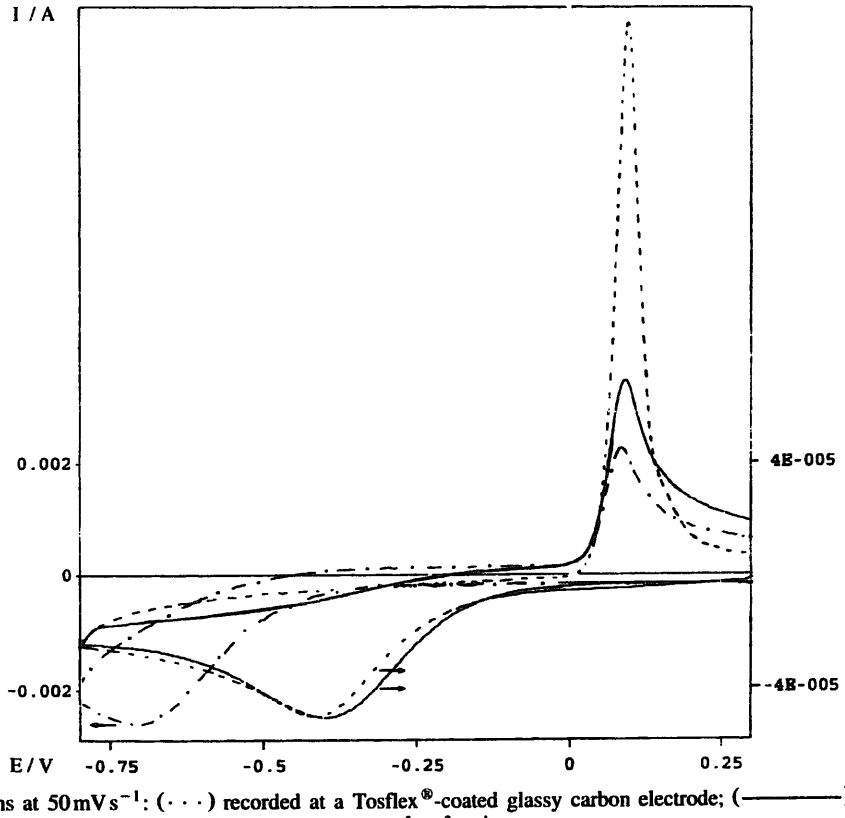

Fig. 4. Cyclic voltammograms at 50 mV s^{-1}: (· · ·) recorded at a Tosflex®-coated glassy carbon electrode; (————) simulated using a diffusion coefficient $D_A = 3 \times 10^{-9}$ cm^2 s^{-1}; (– · –) simulated with $D_A = 1 \times 10^{-5}$ cm^2 s^{-1}.

In order to check such an interpretation, the influence of changes in diffusion coefficients on the voltammetric patterns has been examined by using digital simulation procedures.

Fig. 4 shows that quite satisfactory agreement between simulated (full line, current scale on the right) and experimental data (dashed line, current scale on the right) is achieved by fitting the reactions of Eqs. (2) and (3) with the mechanism

$$A + e^- = B \quad (5)$$

$$B + e^- = C \quad (6)$$

which is optimised by the following values of the model parameters: $E°(5) = 0.300\,V$, $\alpha(5) = 0.35$, $k_s(5) = 8 \times 10^{-9}\,cm\,s^{-1}$; $E°(6) = -0.100\,V$, $\alpha(6) = 0.4$, $k_s(6) = 3 \times 10^{6}\,cm\,s^{-1}$; and $D_A = 3 \times 10^{-9}\,cm^2\,s^{-1}$, $D_B = 1.4 \times 10^{-29}\,cm^2\,s^{-1}$, $D_C = 1.1 \times 10^{-16}\,cm^2\,s^{-1}$.

The experimental curve is obtained operating at an $HgCl_4^{2-}$ solution concentration of 10^{-5} M, while the simulation has been run for a concentration of the species A (which corresponds to $HgCl_{4p}^{2-}$) equal to $10^{-5} k_D = 1.1 \times 10^{-1}$ M.

The $E°$ values are the formal potentials in the coating and do not coincide necessarily with formal potentials in the solution phase [26].

It must be noted that, probably because of the inadequacy of the simulation program in handling the stripping of metal deposits (which are characterised by almost zero diffusion coefficient values and whose formation and dissolution changes the energetics of the relevant redox processes), the simulated stripping peak current is in any case lower than the experimental one.

Focusing on the reduction pattern, it is interesting to note that the increase of D_A to $1 \times 10^{-6}\,cm^2\,s^{-1}$ gives the simulated voltammogram shown in Fig. 4 by the dot dash line (current scale on the left). It is characterised by higher peak currents (which are proportional to $D^{1/2}$) and by a dramatically more negative potential of the reduction peak. Such a shift in the potential of the reduction peak confirms the importance of the diffusion overpotential in ruling changes in peak potential values for irreversible reduction processes.

Unfortunately, the variety and complexity of the phenomena involved in the deposition of metallic mercury at Tosflex®-coated electrodes prevents a fully quantitative evaluation of individual contributions; for these reasons, numerical values obtained by the simulation of voltammograms must be taken as indicative values.

3.2. Oxidation and calomel formation

As shown in Figs. 1 and 3, the potential of peak (b), recorded in the backward scan, changes only slightly with the scan rate and/or the analyte concentration.

The $(E_p - E_{p/2})$ values are always quite small (33 to 38 mV).

The peak current increases linearly with v in the range 5 to 200 mV s^{-1} and with the analyte solution concentration, at least up to 10^{-5} M.

As shown in Fig. 5(A), if a further reduction is performed after the reoxidation scan, at quite high $HgCl_4^{2-}$ solution concentrations a reduction peak (b′), associated with the oxidation peak (b), is observed. When the mercury(II) solution concentration is lowered, the peak (b′) is lowered correspondingly and even disappears as in the case shown in Fig. 5(B).

In order to verify the nature of the solid phases involved in the redox process, ex situ X-ray diffractograms on modified electrodes loaded at quite high Hg(II) solution concentrations (10^{-4} M) have been recorded, both after reduction at −800 mV and after reoxidation at +300 mV; relevant X-ray diffractometric patterns are shown in Fig. 6. Curve (a) shows that the diffractogram recorded after the reduction step does not display any diffraction peak of a crystalline phase apart from the signal relevant to the Teflon support of the electrode mount, which was already present in blank measurements. Comparison with curve (b) shows that the ex situ diffractogram recorded after reoxidation is characterised by a peak at the diffraction angle ($2\theta = 28.3°$) characteristic of the Hg_2Cl_2 crystal lattice [29]. No crystalline deposit was detected when operating at low $HgCl_4^{2-}$ solution concentration ($< 10^{-6}$ M).

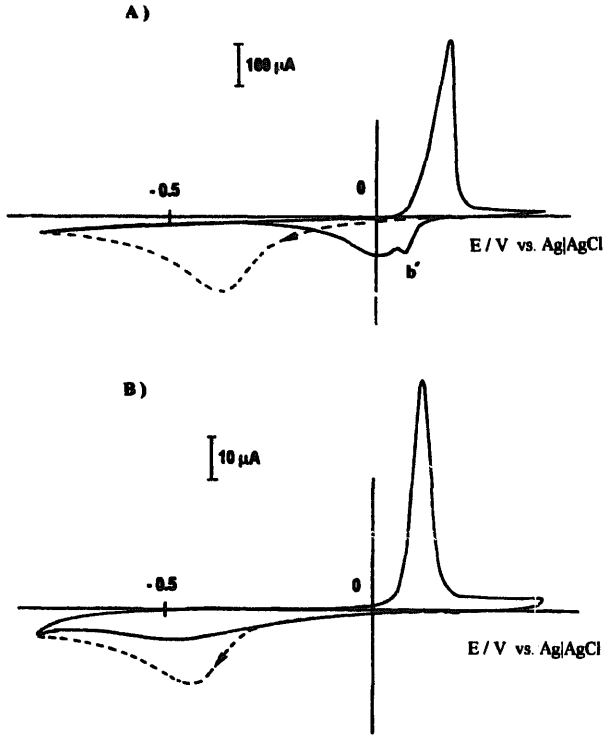

Fig. 5. Cyclic voltammograms recorded at a Tosflex®-coated glassy carbon electrode dipped in Hg(II) solutions 1×10^{-4} M (A) and 5×10^{-6} M (B); (---) first scan from +200 mV to −800 mV; (————) second and third scan from −800 to +400 mV and vice versa. Other experimental conditions as in Fig. 3.

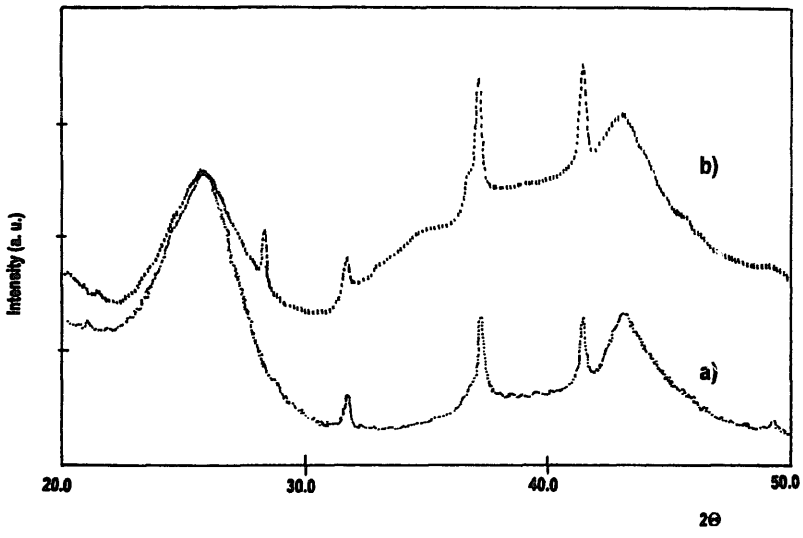

Fig. 6. X-ray diffractogramms of a Tosflex®-coated glassy carbon electrode after equilibration in 10^{-4} M Hg(II) + 0.5 M NaCl + 10^{-2} M HCl and reduction at −800 mV for 10 min (a) and after the reoxidation at +300 mV (b) for the same time.

All this evidence agrees with the involvement at peak (b) of an EC oxidation process composed of the one-electron reversible oxidation of mercury to calomel (see the reaction in Eq. (3)) followed by the disproportionation reaction in Eq. (7):

$$Hg_2Cl_2 + 2Cl^- \rightleftarrows Hg^0 + HgCl_4^{2-} \quad (7)$$

The peak (b′) is the peak associated with the electrochemical reduction of calomel to Hg^0.

It must be emphasised that, unlike the reduction of $HgCl_4^{2-}$, the rate determining step of the charge transfer involved in the reoxidation of Hg^0 to calomel is reversible.

The charge transfer alone is observed at quite high $HgCl_4^{2-}$ loadings, while, at low loadings, also the disproportionation reaction (Eq. (7)) occurs. In the first case, the reoxidation is a one-electron process while in the latter the overall process is a two-electron process.

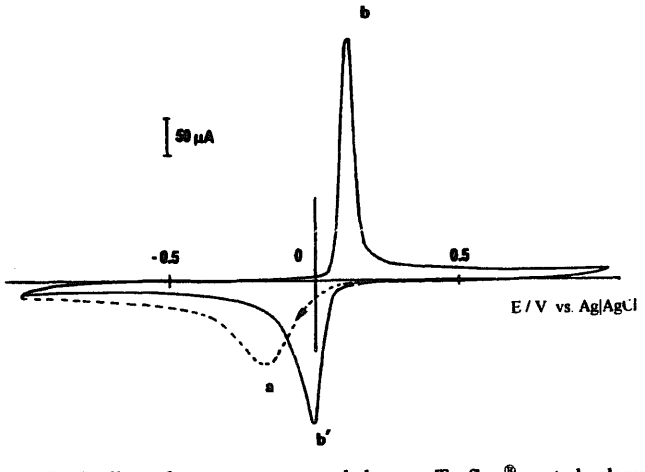

Fig. 7. Cyclic voltammogram recorded at a Tosflex®-coated glassy carbon electrode dipped in 5×10^{-5} M Hg(II) solution, 0.5 M NaCl, in 0.1 M acetate buffer, pH 4.5; scan rate 5 mV s^{-1}: (---) first scan from +200 mV to −1000 mV; (————) second and third scan from −1000 to +1000 mV and vice versa.

Such results can be explained by taking into account that at low $HgCl_4^{2-}$ loadings the great majority of the ion-exchange sites interact directly with Cl^-, which is present within the coating at concentration levels equal to the total concentration of ion-exchange sites, i.e. about 1 M. Such a high local Cl^- concentration favours the disproportionation reaction (Eq. (7)), which is known to be operative in the presence of excess chloride [30].

This is confirmed also by the voltammogram shown in Fig. 7, which is recorded after the addition of acetate to the NaCl supporting electrolyte. The voltammetric pattern is now characterised by a much more relevant height of peak (b′) which is caused by the efficient competition of the acetate anion with Cl^- for the ion-exchange sites of the coating [31]. The decrease in the Cl^- concentration inside the coating makes the disproportionation reaction (Eq. (7)) more difficult.

Values of the areas of peaks (a) and (b) and their relevant ratios measured in the presence of acetate at different Hg(II) solution concentrations are listed in Table 2. These data show that this ratio is lowered progressively by lowering the solution concentration of Hg(II). The evidence that a ratio higher than one is observed at high Hg(II) solution concentrations confirms the involvement of a one electron oxidation at peak (b) and a two-electron reduction at peak (a).

Table 2
Dependence of the ratio of the areas of peaks (a) and (b) on Hg(II) solution concentration, at Tosflex®-coated glassy carbon electrodes; electrolyte solution: 0.5 M NaCl in 0.1 M acetate buffer, pH 4.5; scan rate: 5 mV s^{-1}

[Hg(II)]/M	A_{pA} / A_{pB}
5×10^{-7}	1.18
5×10^{-6}	1.54
1×10^{-5}	1.96

At lower concentrations, the occurrence of the disproportionation reaction (Eq. (7)) increases to two the number of electrons exchanged in the oxidatic . In principle, the occurrence of the disproportionation reaction can influence also the pathway of the reduction process; however, in this case the involvement of the disproportionation does not change the number of electrons exchanged, this being always equal to two.

It is worth noting that in the experimental conditions of the simulations shown in Fig. 4, the role of the reaction in Eq. (7) is negligible. This is confirmed by the evidence that the introduction of this reaction in the mechanism does not change the simulated voltammogram. Moreover, the ratio between the areas under peaks (a) and (b) in the relevant dashed-line experimental voltammogram is close to two, which means that the reoxidation is a simple one-electron process.

The involvement of the reaction in Eq. (7) when operating in dilute $HgCl_4^{2-}$ solutions ($< 10^{-6}$ M) has practical consequences since it indicates that, in this case, the voltammetric reoxidation scan is able to regenerate the modified electrode fully by reoxidizing Hg^0 to $HgCl_4^{2-}$. The achievement of the full regeneration of the modified electrode in dilute solutions has been already observed experimentally [13].

4. Conclusions

This study allowed us to characterise some of the factors which govern the electrochemical behaviour of $HgCl_4^{2-}$ at Tosflex®-coated glassy carbon electrodes.

Concerning the reduction process, the roles played by the slower diffusion rate of the electroactive species within the coating as well as the influence of the coating on the deposition process have been proved.

On the other hand, the study of the reoxidation mechanism has shown the importance of the ion-exchange preconcentration in governing calomel formation and disproportionation.

All experimental evidence obtained supports the occurrence of the overall pathway given by Eqs. (1)–(3) and (7), i.e.

$$2Cl_p^- + HgCl_{4s}^{2-} \rightleftarrows HgCl_{4p}^{2-} + 2Cl_s^- \quad (1)$$

$$2HgCl_{4p}^{2-} + 2e^- \rightarrow Hg_2Cl_2 + 6Cl^- \quad (2)$$

$$Hg_2Cl_2 + e^- \rightleftarrows 2Hg^0 + 2Cl^- \quad (3)$$

$$Hg_2Cl_2 + 2Cl^- \rightleftarrows Hg^0 + HgCl_{4p}^{2-} \quad (7)$$

The Cl^- involved in the reactions in Eqs. (2), (3) and (7) could be both in the solution, s, or polymer, p, phases.

The ion-exchange reaction (Eq. (1)) is the basis of the preconcentration of $HgCl_4^{2-}$ at Tosflex®-coated glassy carbon electrodes. If the coated electrode is dipped in solutions containing $HgCl_4^{2-}$ at concentration levels higher than about 10^{-6} M, the reduction proceeds via reactions in Eq. (2) + Eq. (3) and the reoxidation via the reaction in Eq. (3) alone.

For $HgCl_4^{2-}$ solution concentrations lower than 10^{-6} M, also the disproportionation reaction (Eq. (7)), which is favoured by the high chloride concentration (1 M) existing inside the coating, becomes important. Under such conditions, the reduction can follow the Eq. (2) + Eq. (7) pathway and, eventually, the reoxidation the Eq. (3) + Eq. (7) path.

The information obtained has analytical implications since it allows a more rational choice of experimental conditions in ion-exchange anodic-stripping voltammetry, for optimising both the deposition (reduction) and detection or regeneration (reoxidation) steps.

From a more general point of view, this work has shown that the diffusive contribution to the overpotential which affects irreversible metal plating processes, is dramatically lowered when the reduction is carried out at electrodes coated by ion-exchange membranes instead of using bare solid electrodes.

Acknowledgements

We wish to thank Professor S. Enzo for the X-ray diffractometric measurements and Mr. D. Rudello for technical assistance. This work was supported by MURST (Rome) and CNR (Rome).

References

[1] P. Ugo and L.M. Moretto, Electroanalysis, 7 (1995) 1105.
[2] R. Naegeli, J. Redepenning and F.C. Anson, J. Phys. Chem., 90 (1986) 6227.
[3] A. Fitch, J. Electroanal. Chem., 284 (1990) 237.
[4] J. Redepenning, B.R. Miller and S. Burnham, Anal. Chem, 66 (1994) 1560.
[5] J.-M. Zen and M.-J. Chung, Anal. Chem., 67 (1995) 3571.
[6] Z. Wang, A. Galal, H. Zimmer and H.B. Mark, Jr., Electroanalysis, 4 (1992) 77.
[7] R. Toniolo, G. Bontempelli, G. Schiavon and G. Zotti, J. Electroanal. Chem., 356 (1993) 67.
[8] S. Dong and Y. Wang, Talanta, 35 (1988) 819.
[9] S. Dong and Y. Wang, Anal. Chim. Acta, 212 (1988) 341.
[10] Z. Gao, P. Li and Z. Zhao, Microchem. J., 43 (1991) 121.
[11] G. Schiavon, G. Zotti, R. Toniolo and G. Bontempelli, Anal. Chim. Acta, 264 (1992) 221.
[12] R. Toniolo, N. Comisso and G. Bontempelli, Talanta, 41 (1994) 473.
[13] P. Ugo, L.M. Moretto and G.A. Mazzocchin, Anal. Chim. Acta, 305 (1995) 74.
[14] J.W. Moore and S. Ramamoorthy, Heavy Metals in Natural Waters, Springer, New York, 1984, Chapter 7.
[15] L. Dunsch, L. Kavan and J. Weber, J. Electroanal. Chem., 280 (1990) 313.
[16] C.R. Martin, I. Rubinstein and A.J. Bard, J. Am. Chem. Soc., 104 (1982) 4817.
[17] A.J. Bard and L.R. Faulkner, Electrochemical Methods, Fundamentals and Applications, Wiley, New York, 1980, Chapter 6.

[18] R.W. Murray, in A.J. Bard (Ed.), Electroanalytical Chemistry, Vol. 13, Marcel Dekker, New York, 1984, p. 191.
[19] Kh. Brainina and E. Neyman, Electroanalytical Stripping Methods, Wiley, New York, 1993, Chapters 1 and 2 and references cited therein.
[20] M. Stulikova, J. Electroanal. Chem., 48 (1973) 33.
[21] R. Greef, R. Peat, L.M. Peter, D. Pletcher and J. Robinson, Instrumental Methods in Electrochemistry, Ellis Horwood, Chichester, 1985, Chapter 6.
[22] G. Torsi and G. Mamantov, J. Electroanal. Chem., 32 (1971) 465.
[23] R.W. Andrews, J.H. Larochelle and D.C. Johnson, Anal. Chem., 48 (1976) 212.
[24] C.-H. Chen and A.A. Gewirth, Phys. Rev. Lett., 68 (1992) 1571.
[25] J. Inukai, S. Sugita and K. Itaya, J. Electroanal. Chem., 403 (1996) 159.
[26] P.K. Wrona and Z. Galus, in A.J. Bard (Ed.), Encyclopedia of Electrochemistry of the Elements, Part A, Vol. 9, Marcel Dekker, New York, 1982, Chapter 9.
[27] F. Vydra, K. Stulik and E. Julakova, Electrochemical Stripping Analysis, Ellis Horwood, Chichester, 1976, Chapter 2.
[28] R.G. Dhaneshwar and A.V. Kulkarni, J. Electroanal. Chem, 99 (1979) 207.
[29] JCPDS, Powder Diffraction File, International Center for Diffraction Data, USA, 1978.
[30] F.A. Cotton and G. Wilkinson, Advanced Inorganic Chemistry, Wiley, New York, 5th edn., 1988
[31] F. Helfferich, Ion Exchange, McGraw-Hill, New York, 1962.